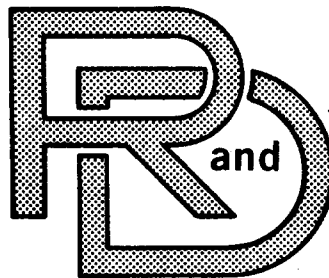


3.14

686

ADA 092 277

AD-A092 277



TARADCOM

LABORATORY

TECHNICAL REPORT

NO. 12522



ANALYTICAL MODEL FOR THE TURNING OF TRACKED  
VEHICLES IN SOFT SOILS

by Leslie L. Karafiath  
Research Department  
Grumman Aerospace Corporation  
Bethpage, New York 11714  
  
Contract DAAK30-78-C-0080

**U.S. ARMY TANK-AUTOMOTIVE  
RESEARCH AND DEVELOPMENT COMMAND  
Warren, Michigan 48090**

BEST AVAILABLE COPY

20000727312

Grumman Research Department RE-

ANALYTICAL MODEL FOR THE TURNING OF  
TRACKED VEHICLES IN SOFT SOILS

Final Report

by

Leslie L. Karafiath

Prepared Under Contract DAAK30-78-C-0080

for


U.S. Army Tank-Automotive Research  
and Development Command  
Warren, Michigan 48090

by

Research Department  
Grumman Aerospace Corporation  
Bethpage, New York 11714

October 1980

Approved by:

  
Richard A. Scheuing  
Director of Research

## FOREWORD

Recent developments in defensive weapons systems make it imperative for the combat and support vehicles of the Army to move on the ground with utmost agility. In the case of tracked vehicles, the speed of turning required for evasive tactics to be successful is often limited by the high turning resistances encountered in soft soils and by the ability of the vehicles to develop the slewing forces necessary to overcome these turning resistances.

Simulation of the interaction of terrain and tracked vehicles in the turning mode is essential to the improvement of the agility of the tracked combat and support vehicles of the Army. The applied mechanics approach developed at Grumman over the years for the solution of wheel-soil and tire-soil interaction problems has been applied to the simulation of the steady state turning of tracked vehicles. Track-soil interaction models, simulating the action of flexible tracks used by the Army, have been developed for the driving mode (outer track in turning) and towed or braking mode (inner track in turning). Interactions occurring in the turning mode between vehicle components and soil, such as load transfer from the inner to the outer track, roadwheel load redistribution due to track forces, offset of the yaw center due to limitations on interface shear stresses, etc., have been taken into account. The analytical turning model developed by the applied mechanics approach is suitable for the parametric analysis of the effect of various design variables on turning performance and offers insight into the various interrelationships that govern the turning performance of tracked vehicles.

## ABSTRACT

An analytical model has been developed for the steady state turning of tracked vehicles in soft soils. The tracks of the vehicle are modeled by a series of rigid plates, each representing track links directly loaded by the roadwheels. The action of the track links in between the directly loaded ones is represented by a surcharge pressure. The soil is modeled by its Coulomb strength parameters; the interface between soil and track is characterized by the interface friction angle and slip.

Track-soil interaction models have been developed separately for the outer track (driving mode) and inner track (braking mode), using plasticity theory for the determination of soil reactions. The slewing forces needed to overcome the turning resistances are determined iteratively. The yaw center offset is determined on the principle that it minimizes the turning resistance. Examples show the applications of the model for the determination of turning resistance, maximum speed of steady state turning and horsepower requirement for various military vehicles and soil conditions.

## ACKNOWLEDGMENT

The work reported herein was performed for the Tank-Automotive Concepts Laboratory of the U.S. Army Tank-Automotive Research and Development command (TARADCOM), Warren, Michigan, under the general supervision of Col. T. Huber, Director of the Laboratory, Mr. Otto Renius, Chief, Survivability Research Division, and Mr. Zoltan J. Janosi, Chief, Applied Research Function. Mr. Zoltan J. Janosi was also technical monitor. Their help and valuable suggestions in carrying out this work are gratefully acknowledged.

## TABLE OF CONTENTS

<u>Section</u>	<u>Page</u>
1 Scope of Work and Objectives. . . . .	1
2 Tracked Vehicle-Terrain Interactions in Turning . . . . .	3
3 Offset of the Yaw Center in Turning . . . . .	7
4 Models of Track-Soil Interaction for the Outer and Inner Track of Vehicles Turning in Soft Soil. . . . .	11
Track-Soil Interaction Model for the Outer Track of Turning Vehicles. . . . .	13
Track-Soil Interaction Model for the Inner Track of Turning Vehicles (Braking Mode) . . . . .	22
5 Turning Model for Soft Soil Conditons . . . . .	25
6 Analyses of Turning Performance in Soft Soil. . . . .	35
7 Conclusions and Recommendations . . . . .	51
8 References. . . . .	53
Distribution List . . . . .	55
Form 1473 . . . . .	59

## LIST OF ILLUSTRATIONS

<u>Figure</u>		<u>Page</u>
1	Load Transfer Due to Centrifugal Forces in Turning. . . . .	4
2	Transverse Shear Stresses Generated at Track Soil Interface in Turning & the Effect of Limitation on Magnitude of These Shear Stresses Imposed by the Available Shearing Resistance . .	9
3	Effect of Slewing Forces on Mode of Track Soil Interaction in Turning . . . . .	12
4	Semi-Rigid Track-Soil Interaction Model for Outer Track of Turning Vehicles. . . . .	14
5	Concept of Interface Friction Angle . . . . .	14
6	Redistribution of Road Wheel Loads Due to Track Forces. . . . .	17
7	Flowchart for Determining $\tan \delta$ -Drawbar Pull Relationship by Semi-Rigid-Track/Soil Interaction Model . . . . .	19
8	Drawbar Pull -- $\tan \delta$ & Track Force -- $\tan \delta$ Relationship for M113 Vehicle in Sand, Track Load = 10,000 lb. . . . .	21
9	Semi-Rigid-Track/Soil Interaction Model for Inner Track of Turning Vehicles. . . . .	23
10	Logic of Analytical Turning Model . . . . .	29
11	Shear Stresses Generated at Track-Soil Interface in Turning . .	32
12	Coefficient of Turning Resistance for M60 Tank at Various Speeds in Soil Condition 2. . . . .	37
13	Variation of Coefficient of Turning Resistance with Soil Conditions for M113 Vehicle at 10 mph . . . . .	39
14	Time Required by the XM1 Tank to Make 90° Turns at Various Radii in Soil Condition 2 . . . . .	40
15	Time Required by XM1 Tank to Make 90° Left & Right Turns in Soil Condition 2. . . . .	41
16	Time Required by Various Vehicles to Make 90°, R = 200 ft Turn in Soil Condition 2. . . . .	43

<u>Figure</u>		<u>Page</u>
17	Time Required by M113 Vehicle to Make 90° Turns in Various Soils . . . . .	44
18	Maximum Speed Attainable by "Hotrod" Version of M113 at Various Radii Under Soil Condition 2. . . . .	45
19	Maximum Speed Along a Sinuous Path, Controlled by Steady State Turning About Instantaneous Radius of Curvature . . . . .	47
20	Sprocket Horsepower Requirements for Sinuous Maneuver Shown in Fig. 19. . . . .	49

#### LIST OF TABLES

<u>Table</u>		<u>Page</u>
1	Input Data for Turning Model . . . . .	27
2	Output Options . . . . .	28
3	Selected Soil Conditions . . . . .	36



## 1 - SCOPE OF WORK AND OBJECTIVES

The main scope of work and objectives of the program are as follows:

- o Development of a track-soil interaction model for the determination of the performance of the outer track of turning vehicles
- o Development of a track-soil interaction model for the determination of the drag exerted by the inner track of turning vehicles
- o Development of a turning model for skid steered tracked vehicles for the prediction and analysis of the maximum speed and power required at various turning radii in soft soils characterized by its Coulomb strength parameters.

## 2 - TRACKED VEHICLE-TERRAIN INTERACTIONS IN TURNING

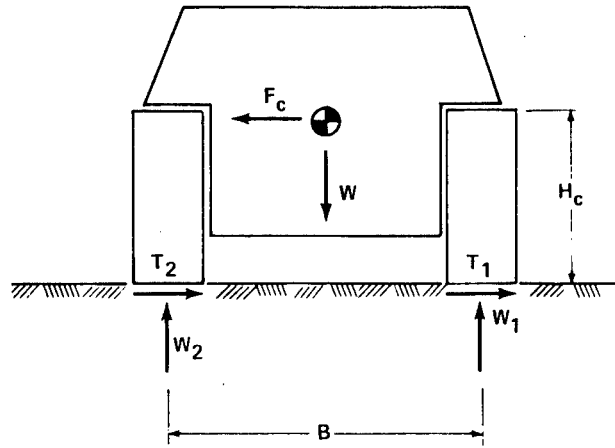
In the development of analytical models for the simulation of the performance of off-road vehicles it is important to recognize the various interactions that take place between vehicle and terrain. In straight line motion the soil response to vehicle loading depends on the characteristics of the vehicle (weight, location of c.g., number of roadwheels, track geometry, etc.) and the interactions between the applied tractive forces and soil. These interactions are brought about in the following ways.

The vertical component of the track force in the ascending part of the track relieves the load on the adjoining roadwheels. The redistribution of roadwheel loads due to track forces affects the soil response and the track forces that depend on the soil response. Thus, an interactive relationship exists among the distribution of roadwheel loads, track forces and soil response.

The track forces generate shear stresses at the track-soil interface that reduce the load supporting capacity of the soil. This reduction is critical beneath the last roadwheel where the load supporting capacity is limited by longitudinal soil failure toward the free surface behind the track. As the load supporting capacity of soil beneath the last roadwheel is decreased with an increase of the track force (that promotes longitudinal soil failure), sinkage of the track beneath the last roadwheel increases resulting in a trimmed position of the track. This in turn increases the soil resistance that has to be overcome by the track force. Thus, there is a strong interaction among track force, track position, soil reactions and sinkage.

In the turning mode there are additional interactions between skid steered tracked vehicles and terrain. These are, in the order of their importance, as follows.

The track load on the outer and inner track changes with the magnitude of the centrifugal force that is a function of the mass, speed and turning radius of the vehicle (Fig. 1). While the interaction between the outer track and



0377-001W

**Fig. 1 Load Transfer Due to Centrifugal Forces in Turning**

soil in turns is essentially the same as in straight line motion in the driving mode, the interaction between the inner track and soil in sharp turns is of a different type since the velocity of the hull at the inner track is higher than the track velocity and, therefore, the inner track is in the towed or braked mode. The significance and consequences of this situation are discussed in detail in Chapter 4.

The shear resistances generated at the track-soil interface by the lateral motion of the tracks constitute the major part of soil resistance to turning that has to be overcome by a slewing force couple. The forward directed slewing force at the outer track calls for additional soil thrust and associated increase in track force while the backward directed slewing force at the inner track reduces and, in the cases of interest from the viewpoint of maneuverability, reverses the soil thrust with an associated decrease or reversal of the track force. These changes in the soil thrust affect the interaction of both the outer and the inner track with the soil directly. The resultant changes in the magnitude of the interface shear stresses affect the sinkage and trim angle of the track and, more importantly, the value of the slip experienced by the outer and inner track. Since both the radius of turn and the velocity of the vehicle depend, among other things, on the value of slip, it is clear that multiple interactions exist among these variables. An additional variable, the yaw center offset, enters these interactions under certain circumstances. Its significance and a concept employed for the determination of its magnitude is discussed in the next chapter.

The vehicle-terrain interactions discussed heretofore refer to steady state, (constant radius and velocity) turns. In non-steady turning motion (radius and velocity varies with time) further interactions take place between vehicle and soil. These are the result of the inertia forces that act on the cg of the vehicle at times of acceleration and deceleration and the inertia moment about the yaw axis that resist changes in the angular velocity of the vehicle that occur as the radius of turning changes. These forces and moments act at the cg in the plane perpendicular to the yaw axis while the balancing forces act at the level of track-soil interface. These forces affect the

distribution of roadwheel loads and the generation of slewing forces and interact with the soil response. The steady state turning model developed under the present contract could be suitably expanded to take these transient interactions into account.

### 3 - OFFSET OF THE YAW CENTER IN TURNING

It has been observed that at relatively small radii and high velocities the center of the turning of tracked vehicles is not in the perpendicular line drawn from the cg of the vehicle but at some distance, called the yaw center offset, forward to that line. The cause of this offset of the yaw center is that the magnitude of the shear stresses generated at any point of the track-soil interface by the centrifugal force and the lateral turning motion of the track is limited by the shear resistance available at the track-soil interface at that point.

The limit of the shearing resistance that can be developed at the track-soil interface may be approximated by the Coulombic linear formula as follows

$$s = a + \sigma_n \tan \varphi_i \leq c + \sigma_n \tan \varphi \quad (1)$$

$a$  = adhesion

$\sigma_n$  = normal stress

$\varphi_i$  = friction angle between track and soil

$c$  = cohesion

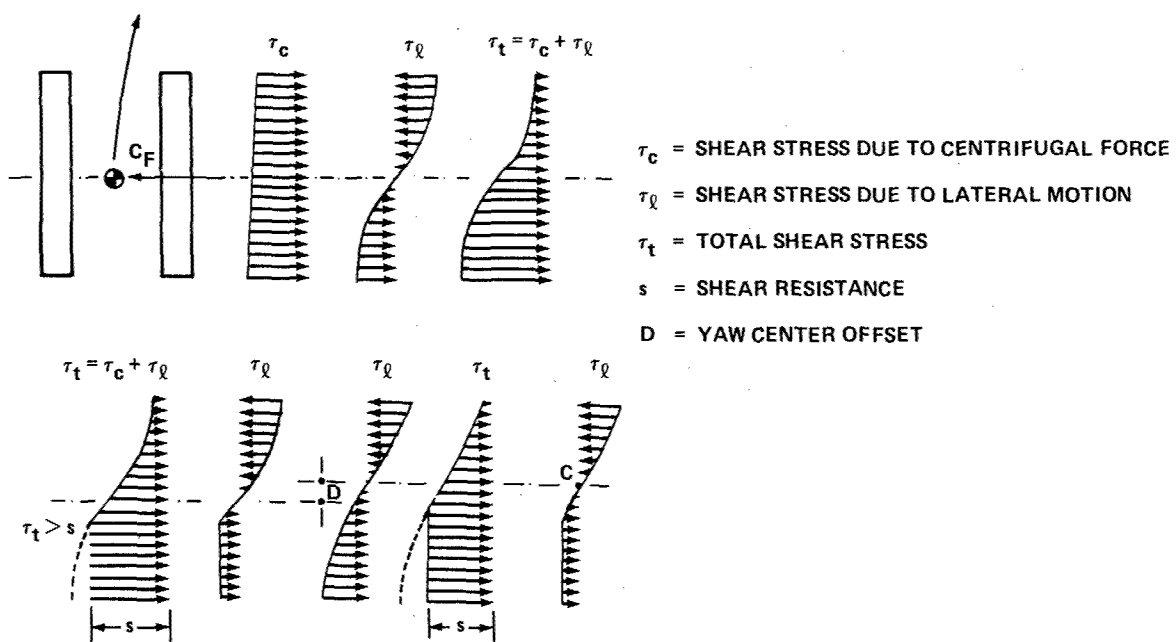
$\varphi$  = friction angle of soil

The total transverse shear stress, the sum of that generated by centrifugal forces and lateral motion, cannot exceed the shearing resistance, as defined by Eq (1), at any point at the track-soil interface. If the sum of the theoretically calculated components of the transverse shear stress is higher than the total shearing resistance then adjustments must be made on the basis of the following considerations. Of the two components of the transverse shear stress the one generated by centrifugal forces is a reaction to these forces, therefore, its value cannot be changed without violating equilibrium conditions. It is the magnitude of the other component, the one generated by the lateral motion of the track, that is reduced if the magnitude

of the total transverse shear stress exceeds the shearing resistance defined by Eq (1). A schematic illustration of the role of the limitation imposed by the shearing resistance on the development of transverse shear stresses is shown in Fig. 2. In the upper part of the figure, the total transverse shear stress as well as its two components are shown separately for the case that the yaw center and cg coincide and the magnitude of total shear stresses does not exceed the available shearing resistance. The turning resistance is the moment of the transverse shear stresses ( $\tau_t$ ) generated by the lateral motion of the track about the yaw center.

In the lower part of Fig. 2, the limiting effect of the shearing resistance on the transverse shear stresses generated by the lateral motion of the track is shown schematically. The shear stress distributions shown in the lower left side of Fig. 2 refer to the case when the yaw center of turning coincides with the cg of the vehicle but the theoretical shear stresses at some locations exceed the shearing resistance. The turning resistance that is the moment of the transverse shear stresses about the yaw center is lower than it would be without the limiting effect of the shearing resistance but it may be higher than the resistance to turning about a yaw center that is located forward of the cg by some distance. A schematic illustration of the transverse shear stress distribution for a yaw center offset of  $D$  is shown in the lower right side of Fig. 2.

The actual magnitude and distribution of shear stresses as well as the available shearing resistance vary along the track and with the location of the yaw center of turning. This variation depends on the interactions that take place between the turning vehicle and soil that have been discussed in the preceding chapter. The location of the yaw center, however, can be determined for any variation of the shear stresses on the principle that of all potential kinematics of shearing the one that offers the least resistance to the applied forces will be the actual one. Thus, the magnitude of the offset of the yaw center is determined on the basis that it always minimizes the turning resistance, all other things being equal.



0377-002W

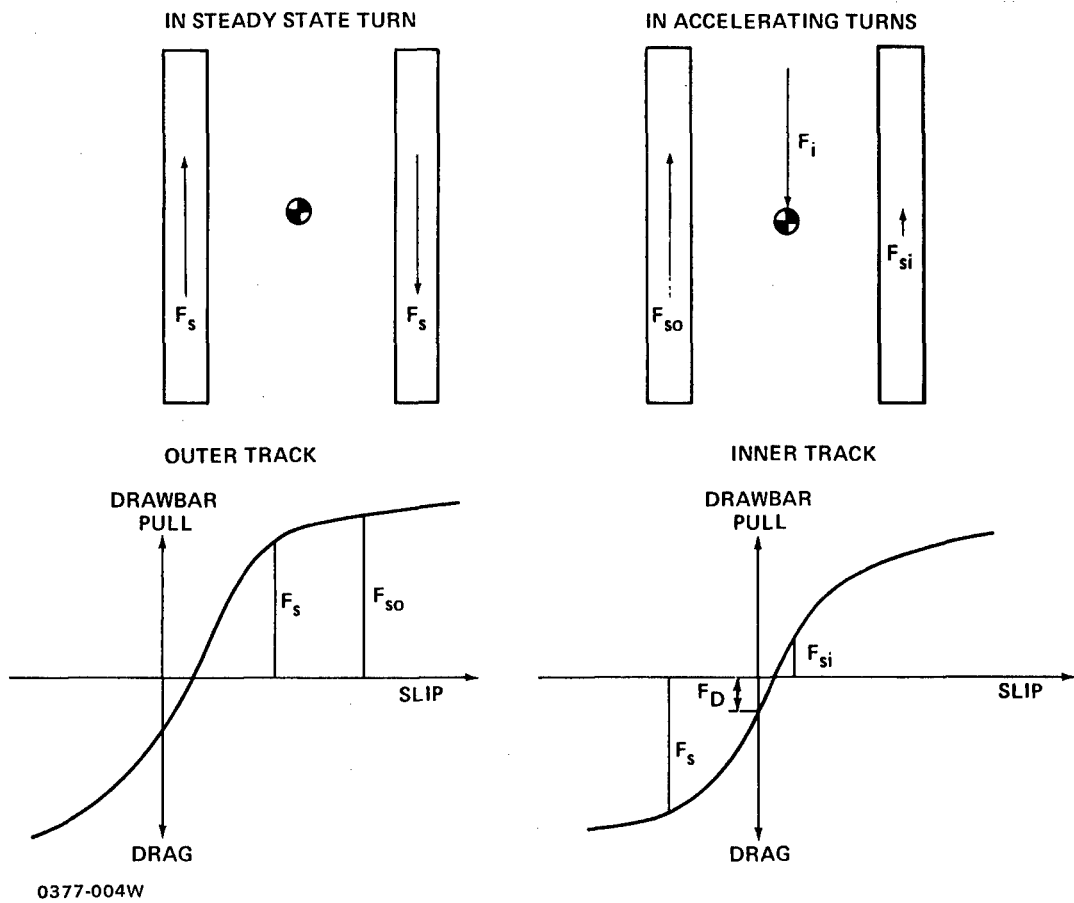
**Fig. 2 Transverse Shear Stresses Generated at Track Soil Interface in Turning & the Effect of Limitation on Magnitude of These Shear Stresses Imposed by the Available Shearing Resistance**



#### 4 - MODELS OF TRACK-SOIL INTERACTION FOR THE OUTER AND INNER TRACK OF VEHICLES TURNING IN SOFT SOIL

The turning of tracked vehicles is effected by a steering mechanisms that enables the driver to control the relative speed of the outer and inner tracks. In this process, a slewing force couple, necessary to overcome the turning resistance, is generated, in addition to the tractive forces necessary to overcome the straight motion resistances. The forward directed slewing force at the outer track requires the development of an additional tractive force, while at the inner track the development of a backward directed slewing force requires a reduction of the tractive force. Depending on the magnitude of this reduction, the inner track may exhibit a positive slip (driving mode) or a negative slip (towed or braking mode). A schematic illustration of these conditions is shown in Fig. 3. In steady state turns the equilibrium of longitudinal forces requires that the slewing force at the inner track be equal and opposite to that developed by the outer track. In fast and sharp turns that are of interest from the viewpoint of agility, large slewing forces need to be developed to overcome the high turning resistances. To develop such large slewing forces, the inner track must generally be in the negative slip range, i.e. in the towed or braking mode (see diagram in the lower right side of Fig. 3). Only if a slewing force smaller than  $T_d$ , shown in Fig. 3, is needed, is the inner track in the driving mode.

In an accelerating turn the situation is different, since the inertia force acting on the cg of the vehicle enters into the equilibrium condition of longitudinal forces. Under accelerating conditions, the inner track is in the driving range for a wide range of slewing and inertia forces (Fig. 3). This is emphasized here because in field testing it is exceedingly difficult to insure steady state conditions assumed in the analytical turning model and field measurements in the transient condition may yield results that are far from comparable to the steady state analysis.



0377-004W

Fig. 3 Effect of Slewing Forces on Mode of Track Soil Interaction in Turning

These considerations show that the interaction between the inner track and soil is fundamentally different from that experienced in straight forward motion. For the purposes of the turning model, separate models of track-soil interaction have been developed for the outer track (driving mode) and the inner track (towed or braking mode) to take into account the effect of slewing forces, as discussed previously.

#### TRACK-SOIL INTERACTION MODEL FOR THE OUTER TRACK OF TURNING VEHICLES

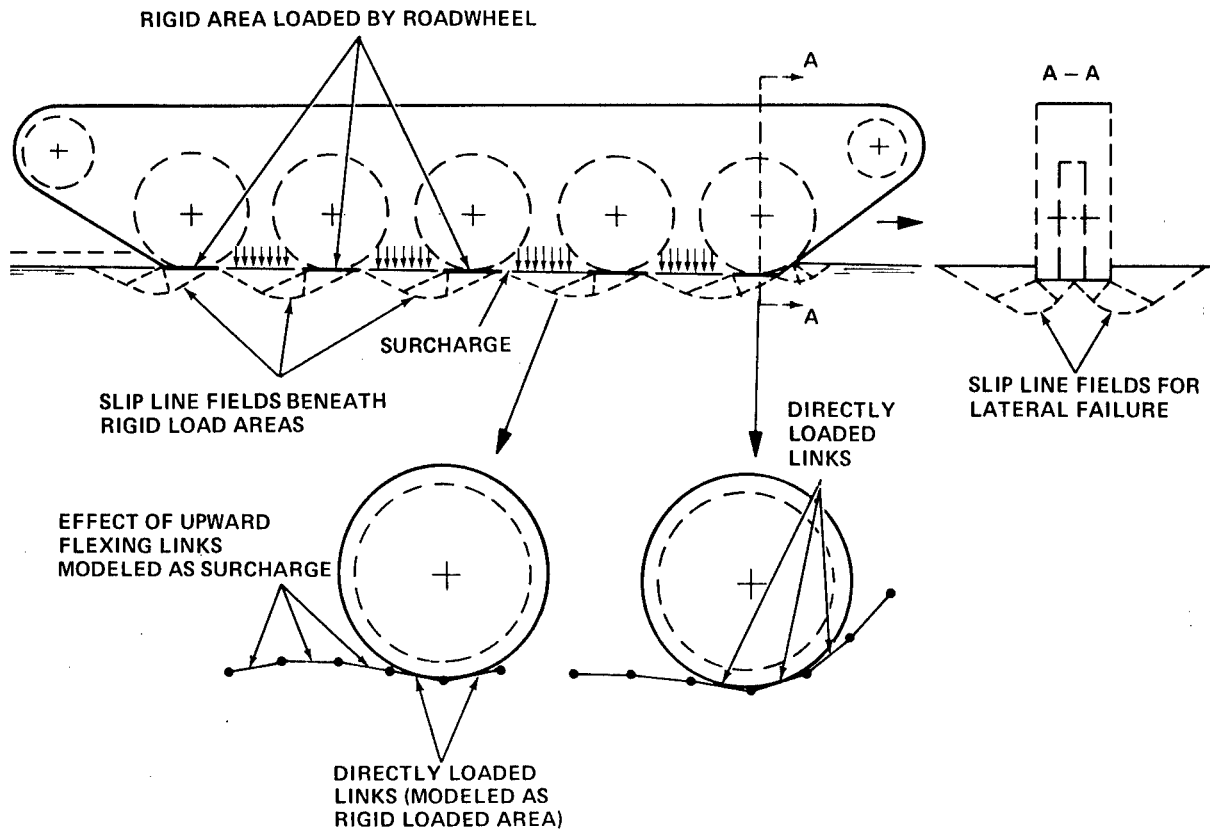
For the determination of the maximum soil thrust that tracked vehicles can develop in soft soil, a rigid track-soil interaction model has been developed under an earlier contract (Ref 1). Analytical studies reported in Ref 1 showed that modeling of the track by a rigid geometry results in interface normal stress distributions different from that experienced with pin-jointed flexible military tracks. A semirigid-track/soil interaction concept was proposed to improve the simulation of the action of flexible tracks. Under this contract the concept was further developed and an analytical model, described in detail below, was prepared.

The semirigid-track/soil interaction model for the outer track, shown schematically in Fig. 4, incorporates the following features.

The soil is modeled by its Coulomb strength parameters (cohesion and friction angle) and its unit weight.

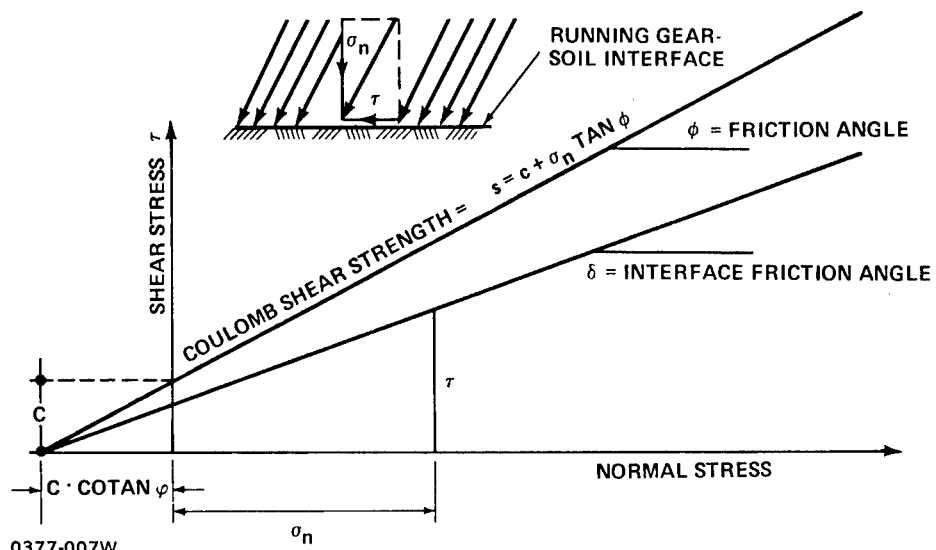
The track is modeled by rigid plates underneath each roadwheel. The size of the rigid plates corresponds to the number of track links directly loaded by the roadwheel. The effect of that part of the track that is between the rigid plates is modeled by a uniform surcharge pressure, the minimum value of which is the weight of the track per the area of contact.

The transfer of stresses at the track-soil interface is modeled by the interface friction angle,  $\delta$  defined as shown in Fig. 5.



0377-006W

Fig. 4 Semi-Rigid-Track/Soil Interaction Model for Outer Track of Turning Vehicles



0377-007W

Fig. 5 Concept of Interface Friction Angle

The maximum value of the interface friction angle,  $\delta_{\max}$ , is the friction angle between track and soil,  $\phi_i$ , that for most military tracks equals the friction angle of soil. Note that the use of the  $\delta$  angle for modeling the transfer of stresses between track and soil implies that the adhesion part of the shear stress also develops in proportion to the tangent of that angle.

The basic concept underlying this model is that under the action of tractive forces shear zones develop in the soil underneath each rigid plate representing the links directly loaded by the roadwheels (Fig. 4). The most critical condition occurs beneath the last roadwheel where the shear zones emerge at the free surface in the rut behind the track. The shear zones underneath the other roadwheels surface beneath the unloaded portions of the track where, in addition to the pressure exerted by the weight of the track, counterbalancing pressures are generated by the soil moving against the track or vice versa. If the soil strength is such that there is no shear failure beneath the last roadwheel, even when the highest track force is applied, then "hard surface" conditions exist and the model is not applicable.

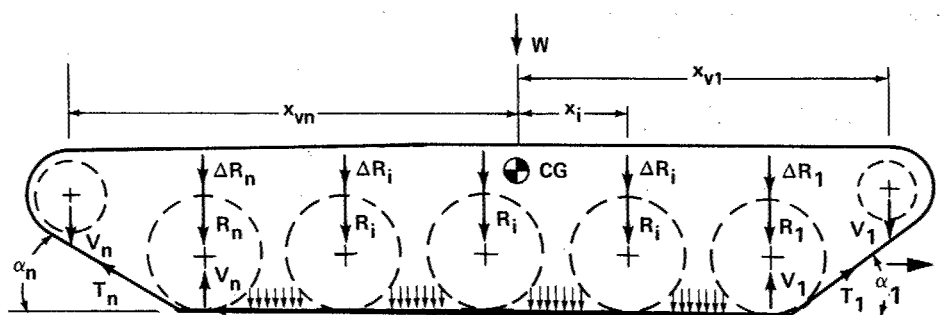
The shear zones initiated by tractive forces are in the plane of travel. There is another mode of shear failure, lateral failure, perpendicular to the plane of travel, that imposes a limitation on the interface normal stresses that sustain the track load. Slip lines, or shear zones for lateral failure, are shown in the right side of Fig. 4. To determine which mode of soil failure is critical it is necessary to determine the interface normal stresses for each mode of failure. Whichever mode of failure yields a lower interface normal stress for a point of the track-soil interface that mode of failure is critical for that point. Generally, lateral failure conditions affect track-soil interaction in cohesionless soils more than in cohesive soils.

The applied track forces affect track-soil interaction not only through their effect on soil response but also by bringing about a redistribution of

roadwheel loads. The vertical component of the track force in the ascending portions of the track relieves the load on the first and last roadwheels and transmits this vertical load component to the drive sprocket and idler wheel, respectively, as shown in Fig. 6. This redistribution of roadwheel loads due to track forces is determined on the assumption that the roadwheel loads vary linearly and the moment about the cg due to this redistribution is zero. In the calculations the effect of sag in the upper returning part of the track and the upward flexing of the track between the roadwheels is neglected.

The redistribution of roadwheel loads due to changes in the track force is interactively incorporated in the calculation of the load carrying capacity of the soil beneath the roadwheels. The track beneath the last roadwheel is modeled by a horizontal rigid plate (representing two links of the track) and an adjoining ascending part that is also loaded directly by the last roadwheel. The height of this ascending part is assumed to be one tenth of the total sinkage, approximately corresponding to the rebound of the soil from the track load. Although in the longitudinal failure mode the slip line field ends at the free surface in the rut where, theoretically, soil failure is not restrained, in reality the rut depth exerts a restraining effect on soil failure. In the model this effect is assumed to be equivalent to a pressure corresponding to the weight of a soil layer half the height of the rut.

The track underneath the first roadwheel is modeled by a horizontal rigid plate (corresponding to two links in the track) and an adjoining ascending rigid portion. The interface normal stresses underneath the first roadwheel are controlled by three potential failure modes: two in the longitudinal plane (one directed backward the other one forward as shown in Fig. 4) and lateral failure in the transverse plane. Of the two longitudinal failure modes, the backward directed applies to the horizontal portion and the forward directed to the ascending portion of the rigid plate. However, it is possible, that at the edge of the rigid plate adjoining the ascending portion of the track and for some distance along the horizontal section, normal stresses from a forward directed failure would be lower than those



**ROADWHEEL LOAD DISTRIBUTION  
WITHOUT TRACK FORCES**

$$\sum_{i=1}^n R_i = W$$

$$\sum_{i=1}^n R_i x_i = 0$$

0377-008W

**EFFECT OF TRACK FORCES**

$$V_n = T_n \sin \alpha_n \quad V_1 = T_1 \sin \alpha_1$$

$$\sum_{i=1}^n \Delta R_i = V_n + V_1$$

$$\sum_{i=1}^n \Delta R_i x_i = V_n x_{vn} + V_1 x_{v1}$$

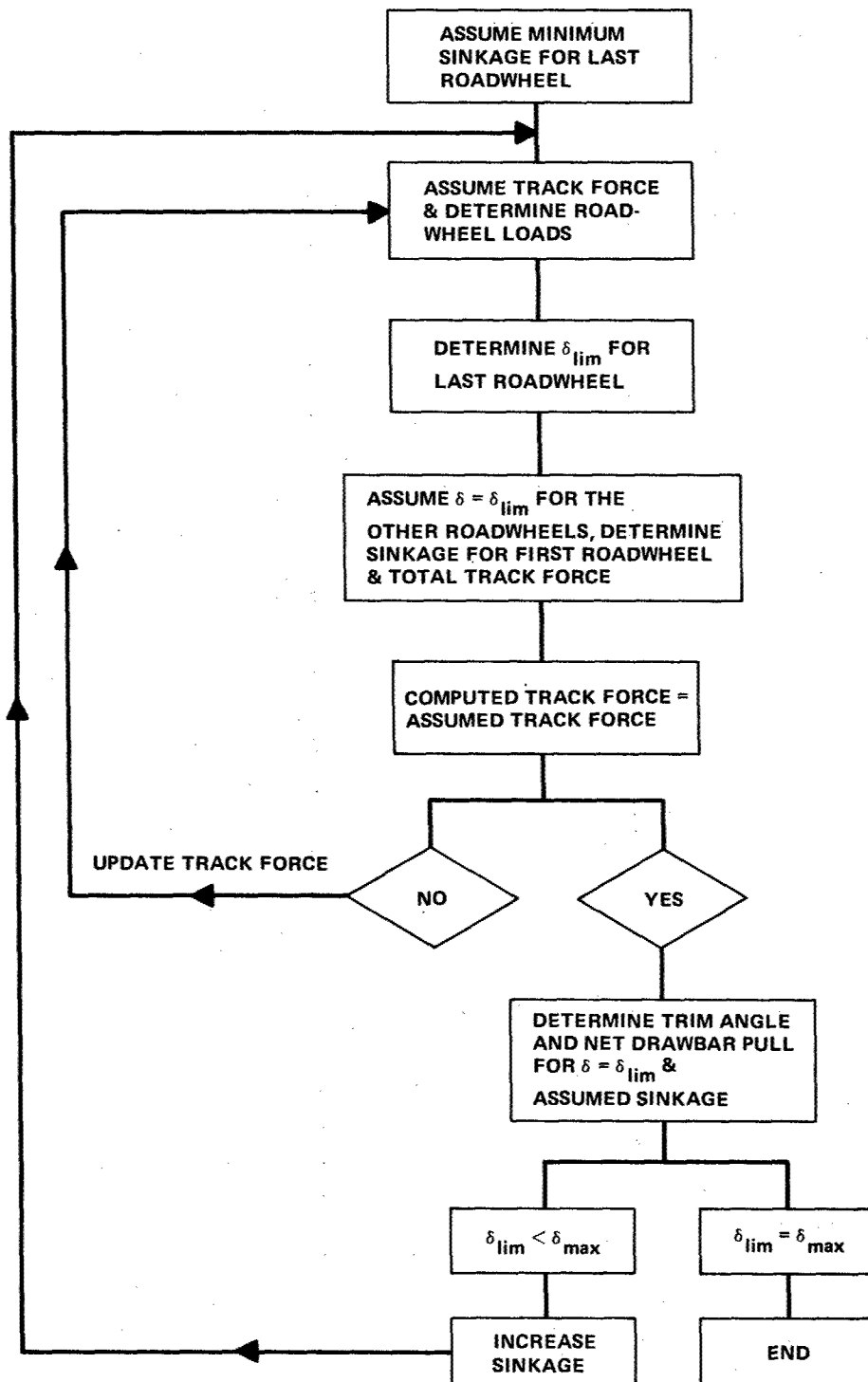
**Fig. 6 Redistribution of Road Wheel Loads Due to Track Forces**

computed for backward directed failure. For this reason in this area interface normal stresses for all three potential failure modes are computed, the lowest of them being accepted as the maximum that can be developed under the given conditions.

In the model the limiting value of the interface friction angle,  $\delta_{lim}$ , is determined on the basis of the critical conditions obtained beneath the last roadwheel. The value of  $\delta_{lim}$  is also a function of the sinkage of the last roadwheel. The conditions beneath the first roadwheel are less critical, therefore, the sinkage pertaining to the same  $\delta_{lim}$  value will be generally less than that at the last roadwheel. In the model the differential sinkage between the first and last roadwheel defines the trim angle. Although the trimmed position affects somewhat the development of shear zones and the interface normal stresses computed therefrom, this effect is deemed negligible, and, therefore, no interactive recomputation of the interface normal stresses has been included in the model. However, the tangential component of the track load resulting from the trimmed position (which often constitutes a major part of the motion resistance) is taken into account in the determination of the net drawbar pull.

In the model, values of  $\delta_{lim}$  for various sinkages beneath the last roadwheel are determined for an assumed track force. It is assumed that the same interface friction angle develops beneath the other roadwheels. If soil failure conditions beneath any of the roadwheels require a balancing counterpressure, then the magnitude of that counterpressure is iteratively determined. Tractive forces developed underneath each roadwheel are determined and summed. If the total tractive force differs from the assumed track force by more than the allowable tolerance, the computation is repeated with an updated value of the track force until satisfactory agreement between the assumed track force and computed values of the total tractive force is reached. Slip values are related to the interface friction angle,  $\delta$ , by the following relation





0377-009W

Fig. 7 Flowchart for Determining  $\tan \delta$ -Drawbar Pull Relationship by Semi-Rigid-Track/Soil Interaction

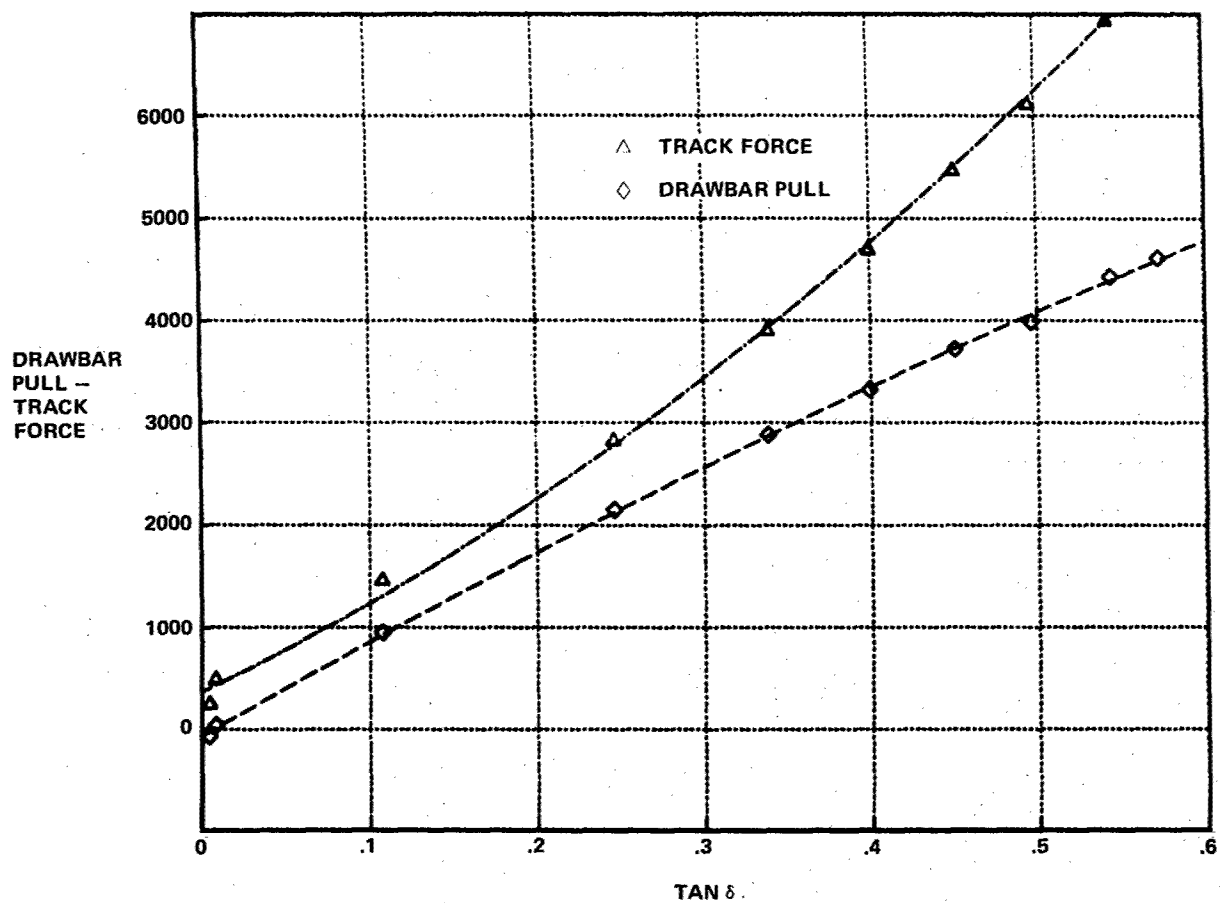
$$\tan \delta = \tan \delta_{\max} (1 - e^{s/K}) \quad (2)$$

where  $s$  = slip

$K$  = slip parameter.

Figure 7 shows the flow chart for the computation of the drawbar pull-tan  $\delta$  relationship for given load and soil conditions. In the turning model drawbar pull-tan  $\delta$  relationships are needed for track loads ranging from the static track load to a theoretical maximum of twice that load. For this purpose it is expedient to use parabolic curve fits to relationships determined for selected trackloads and use interpolation procedures for trackloads other than the selected ones. An example of drawbar pull-tan  $\delta$  and track force-tan  $\delta$  relationships and parabolic curve fits is shown in Fig. 8 for the following conditions:

Track load:	10,000 lb	
Track ground contact length:	8.75	width: 1.25 ft
No. of roadwheels:	5	
Distances from cg:	4.35, 2.17, -2.02, -2.21, -4.42	ft
Distance of drive sprocket from cg:	-6.67	ft
Distance of idler wheel from cg:	6.5	ft
Approach angle:	30°	
Angle of departure:	20°	
Pitch:	.5	ft
Coefficient of internal track resistance:	.04	
Soil cohesion:	.1	lb/sq ft
Soil friction angle:	35°	
Soil unit weight:	100	lb/cu ft
Slip coefficient:	.2	



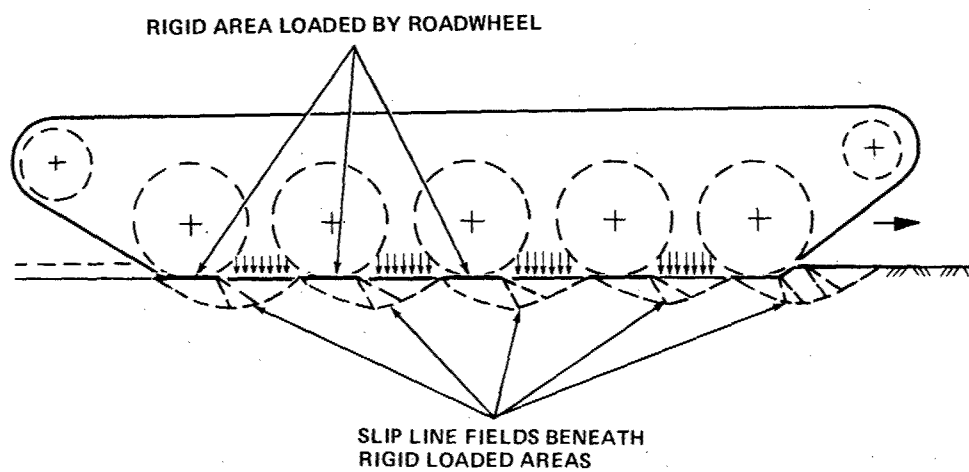
0377-010W

Fig 8 Drawbar Pull -  $\tan \delta$  & Track Force -  $\tan \delta$  Relationship for M113 Vehicle in Sand,  
Track Load = 10,000 lb

## TRACK-SOIL INTERACTION MODEL FOR THE INNER TRACK OF TURNING VEHICLES (BRAKING MODE)

The modeling of track and soil as well as the basic concepts of their interaction are essentially the same for the inner track as for the outer track, discussed in detail in the preceding pages. The direction of the shear stresses at the track-soil interface is, however, reversed, bringing about a different role for the various roadwheels and mode of soil failure associated with it, as illustrated in Fig. 9.

In the case of the inner track soil conditions beneath the first roadwheel are critical, where the forward directed longitudinal failure zones emerge at the virgin surface in the front of the track. Soil failure underneath the other roadwheels would result in a rise of counterbalancing pressures exerted by the upward flexing portions of the track, therefore, plastic equilibrium conditions in the soil can be maintained for practically any load without further sinkage. Beneath the first roadwheel the load supporting capacity of the soil depends on the sinkage. The limiting value of the negative interface friction angle is determined as the one causing plastic failure conditions in the soil beneath the first roadwheel; its value varies with the sinkage of the first roadwheel. Conditions beneath the other roadwheels are not critical, therefore, the sinkage equals the rut depth and the trim angle is zero.



0377-011W

Fig. 9 Semi-Rigid-Track/Soil Interaction Model for Inner Track of Turning Vehicles

## 5 - TURNING MODEL FOR SOFT SOIL CONDITIONS

The track-soil interaction models for the outer and inner track of turning vehicles, described in the preceding section, are the principal components of the model that has been developed for the simulation of the steady state turning of tracked vehicles in soft soil. This model is suitable for the determination of turning resistances at various turning radii and speeds. In conjunction with an appropriate power train and steering transmission model it can be used for the determination of the maximum speed that tracked vehicles are capable of attaining in soft soils at various turning radii.

The turning speed of tracked vehicles may be limited by any of the following conditions:

- 1) Resistance of the soil against skid out is insufficient, i.e., the centrifugal force is greater than the sum of the resistances developed at the track-soil interfaces and the side faces of the tracks.
- 2) Soil thrust that the outer track is capable of developing under the loading conditions of turning is insufficient to generate the slewing force necessary to overcome the turning resistance.
- 3) Soil drag that the inner track is capable of developing under the loading conditions of turning is insufficient to provide the counterbalancing slewing force at the inner track.
- 4) Engine power is insufficient to provide the tractive and slewing forces necessary for turning at the given speed.
- 5) Steering mechanism is incapable of providing the steering ratio and track forces at the track velocities required to execute the turn with the given speed.

The turning model prepared under this contract is directed toward the determination of the tractive and braking forces and turning resistances arising under various soil conditions. Modeling of the power train and steering mechanism, which is outside the scope of this contract, has been included in the model in a simplified form and only for a controlled differential type steering mechanism, such as that of the M113. A simple hyperbolic relation between available track force and speed is assumed and the effect of the steering mechanism on the sprocket horsepower is considered by computing the power loss from the appropriate Merritt formula.

The turning model takes into account the various interactions between vehicle and soil, discussed in Chapter 2, in the following way. The input data that characterize the vehicle and soil conditions in the model are listed in Table 1. The various forms of output that can be specified are listed in Table 2 together with input specifications regarding the range and increments of radii and speed for which the output information is desired. The solution of the problem for any of the specified output forms is based on the determination of the turning resistance for a given radius and speed; the logic of the computations is shown schematically in Fig. 10 and is explained in more detail subsequently. Since the load on the outer and inner tracks vary with the speed and the radius of turning, each combination of the radius and speed represents an individual case. Since the computation of drawbar pull and drag for a particular track load requires considerable computer time, it was found expedient to establish the drawbar pull- $\tan \delta$  and track force- $\tan \delta$  relationships for the outer track and the drag- $\tan \delta$ , track force- $\tan \delta$  relationships for the inner track for the whole range of the variation of track loads. In the model this is accomplished by determining these relationships for selected track load increments (using the track-soil interaction models described in Chapter 4) and establishing parabolic curve fits (such as shown in Fig. 8) for each of these relationships. The determination of  $\tan \delta$  that needs to be developed at the outer and inner track-soil interface for the required drawbar pull and drag, respectively, becomes then a matter of a simple interpolation between parabolic curve fits.

TABLE 1 - INPUT DATA FOR TURNING MODEL

VEHICLE CHARACTERISTICS

Gross weight  
 Tread  
 Ground contact length of track  
 Width of track  
 Height of side face of track  
 Track pitch  
 Entry angle  
 Angle of departure  
 Horizontal distance of cg from last roadwheel axis  
 Height of cg  
 Distance of sprocket drive from cg (+ forward)  
 Distance of idler wheel from cg  
 Weight of track per unit contact area  
 Initial track tension  
 Number of roadwheels on one side  
 Distances of roadwheels from cg on left and right side  
 Coefficient of internal track resistance\*  
 Coefficient of internal track resistance in curves and reference radius\*  
  
 Optional with controlled differential steering:  
  
 Track force - velocity parameters  
 Maximum steering ratio

SOIL CHARACTERISTICS

Cohesion  
 Friction angle  
 Unit weight\*  
 Slip parameter K\*

\*if unknown model assumes default value



TABLE 2 - OUTPUT OPTIONS

I Turning resistance coefficient vs radius and speed

II Time to make 90° turn vs radius and sprocket HP/ton

III Maximum speed vs radius

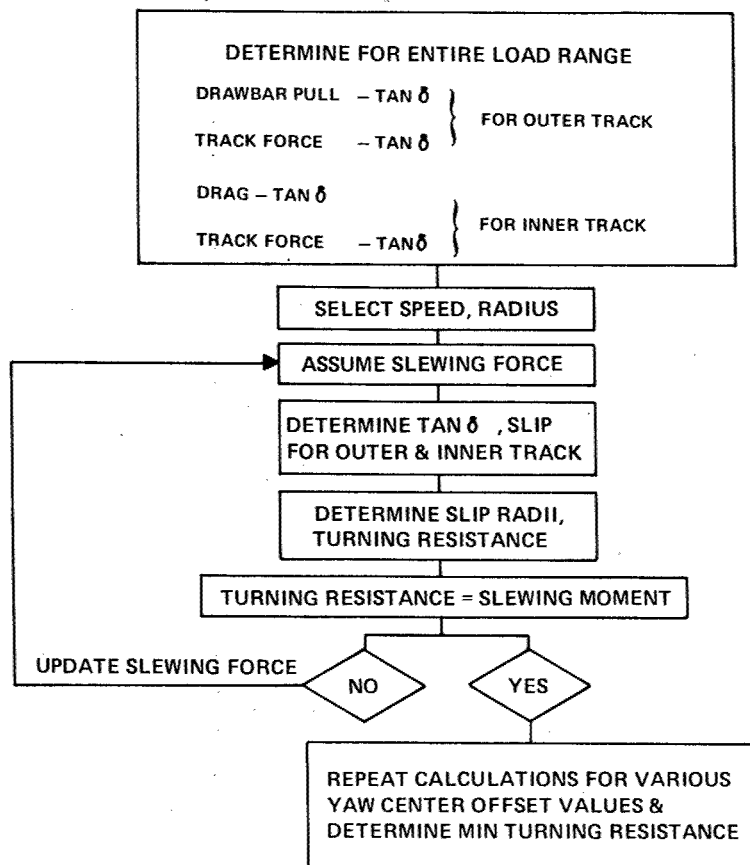
For output options I - III specify:

Minimum radius, radius increment, max. number of increments

Minimum speed, speed increment, max. number of increments

IV Maximum speed in sinuous maneuver

Specify: entry speed, minimum speed, speed increments,  
wavelength and amplitude of sinuous path



0377-012W

Fig. 10 Logic of Analytical Turning Model

With these relationships established, the sequence of computations and iterations necessary to account for the various interactions between vehicle and soil is as follows.

The centrifugal force for the given radius and speed is computed and the load on the outer and inner track is determined, assuming the yaw center offset is zero. A roadwheel load distribution is computed for the assumption that the track force is zero. It is assumed that this roadwheel load distribution approximates the mass distribution of the vehicle. The centrifugal force acting on the cg of the vehicle is thought to be composed of components that act at the location of roadwheels and are proportional to the static roadwheel loads. Shear resistances generated by centrifugal forces are assumed to follow the distribution of the centrifugal force components, irrespective of the changes in roadwheel load distribution due to track forces.

A trial value is assigned to the slewing force. Since the drawbar pull- $\tan \delta$  and drag- $\tan \delta$  relationships obtained from the track-soil interaction models refer to net values of drawbar pull and drag, the  $\tan \delta$  values that need to be developed at the outer and inner track, respectively, may be immediately obtained from these relationships by equating the drawbar pull and drag with the slewing force. The track forces corresponding to these  $\tan \delta$  values are obtained directly from the track force- $\tan \delta$  relationships. Roadwheel loads are recomputed, taking into account the effect of track forces. The longitudinal shear stresses ( $\tau_x$ ) are computed for each roadwheel and intra-roadwheel track area location. The longitudinal slip is determined from the following equation:

$$\tau_x = \tau_{\max}(1 - e^{-s/K}) \quad (3)$$

where  $\tau_{\max}$  = shear stress for  $\delta = \delta_{\max} = \varphi$

$K$  = slip parameter

$$s = \text{slip} = \frac{|V_{th} - V_a|}{|V_{\max}|} = \frac{|V_s|}{|V_{\max}|} \quad (4)$$

where  $V_s$  = slip velocity  
 $V_{th}$  = theoretical velocity = track velocity  
 $V_a$  = actual (travel) velocity  
 $V_{max} = \max (V_{th}, V_a)$

The above definition of slip makes it possible to use the same shear stress-slip relationship for both the outer and inner track and eliminates the problem arising from slip values becoming negative and higher than unity for the inner track.

The slip radius for the outer and inner track is determined from the angular velocity ( $\omega$ ) of the vehicle as

$$r_o = \frac{V_{so}}{\omega}, \quad r_i = \frac{V_{si}}{\omega} \quad (5)$$

(the subscript o denotes outer, i inner track)

The lateral shear stress for each roadwheel and intra-roadwheel area location is determined on the basis that the shear stress,  $\tau$ , generated by the motion of the track relative to the ground, must be colinear with the instantaneous slip velocity ( $V_i$ ) and its longitudinal component must equal  $\tau_x$  (Fig. 11).

The magnitude of the shear stresses generated at the track-soil interface is limited by the shearing resistance that can be developed at that interface. The total shear stress at any point at the interface consists of that generated by the turning motion of the track and that generated by centrifugal forces

$$\bar{\tau}_{tot} = \bar{\tau} + \bar{\tau}_c \quad (6)$$

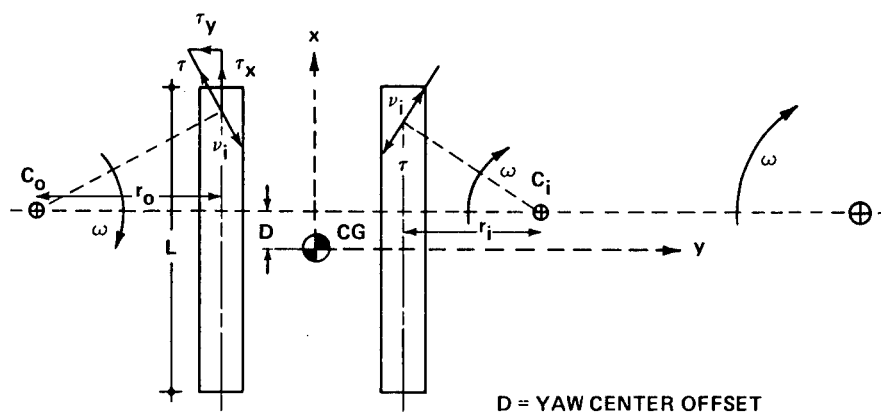
The magnitude of the shear stress vector

$$\tau_{tot} = \sqrt{(\tau_y + \tau_c)^2 + \tau_x^2} \quad (7)$$

is limited by the shearing resistance so that

$$\tau_{tot} \leq c + \sigma_n \cdot \tan \varphi \quad (8)$$

at any point on the interface. If this limitation applies then the



0377-014W

**Fig. 11 Shear Stresses Generated at Track-Soil Interface in Turning**

magnitude of the components in Eq (7) must be reduced so that their sum meets Eq (8). Of the components in Eq (7), only  $\tau_y$  may be reduced since  $\tau_c$  must balance the centrifugal forces and  $\tau_x$  is needed for traction. Thus, the lateral shear resistance to turning is decreased whenever the total shear stress exceeds the available shearing resistance.

The moment of the lateral shear stresses and the shear resistances arising at the side faces of the track (Ref 1) is computed and compared with the slewing moment corresponding to the assumed slewing force. If they differ by more than the allowed tolerance, the computation is repeated with an updated slewing force until the moment of lateral shear resistances matches the slewing moment.

These computations yield the turning resistance for the assumption that the yaw center and cg coincide. The effect of a yaw center offset on the turning resistance is then determined by computing the turning resistances for selected increments of the yaw center offset and determining the yaw center offset that minimizes the turning resistance. The minimum of the turning resistance is accepted as its true value.

In the analytical model the interface stresses that act on the vehicle as a free body are determined by plasticity theory methods and interface shear - slip relations. Those components of the interface stresses that resist motion comprise the external motion and turning resistances. In addition to these, there are internal track resistances, such as friction in joints, angular displacements of bushings, scrubbing of roadwheels against guides, etc., that have to be taken into account when computing sprocket horsepower requirements. For this purpose, a coefficient of internal resistance is defined as follows:

$$C_i = C_{is} + C_{it} \cdot R_c/R \quad (9)$$

where  $C_i$  = coefficient of internal resistance  
 $C_{is}$  = coefficient of internal resistance in straight motion  
 $C_{it}$  = coefficient of internal resistance in turning  
 $R_c$  = reference (minimum) radius of turning  
 $R$  = radius of turning

## 6 - ANALYSES OF TURNING PERFORMANCE IN SOFT SOIL

The analytical turning model described in the preceding section is suitable for various kinds of parametric and comparative analyses of turning performance. The effect of changes in vehicle characteristics, such as cg location, track width, number of roadwheels, etc. on turning performance may be analyzed under various soil conditions for existing vehicles as well as for conceptual vehicles in the design stage, provided all input data are available. Comparative analyses of the turning performance of various tracked vehicles is another area where the model is useful. In view of the great number of combinations of the variables that affect turning performance, it is not practical to show all types of analyses of turning performance that may be of interest. Sample analyses of turning performance, presented subsequently in this section, are illustrations of the capabilities of the model rather than results of extensive parametric analyses.

A measure of the soil resistances that impede the turning of tracked vehicles is the slewing moment that the vehicle must develop if these resistances are to be overcome. The calculation of slewing moment is an integral part of the analytical model. However, a meaningful appreciation of the magnitude of the slewing moment requires that it be related to the characteristics of the vehicle. For this purpose the "coefficient of turning resistance" is introduced. This coefficient, designated in this report as  $\mu_r$ , is defined as follows:

$$\mu_r = \frac{S_M}{\frac{1}{2} GCW \cdot B} \quad (10)$$

where  $S_M$  = slewing moment  
GCW = gross weight of vehicle  
B = track tread

The coefficient of turning resistance, as defined by Eq (10), is conceptually similar to the coefficient of motion resistance. Both define the

ratio of resisting forces to the weight of vehicle. Thus, the coefficient of turning resistance, comparable in magnitude to the motion resistance, is expected to illustrate the magnitude of turning resistance to off-road vehicle engineers more meaningfully than actual values of the slewing moment.

Sample analyses were limited to three soil conditions defined in Table 3 below.

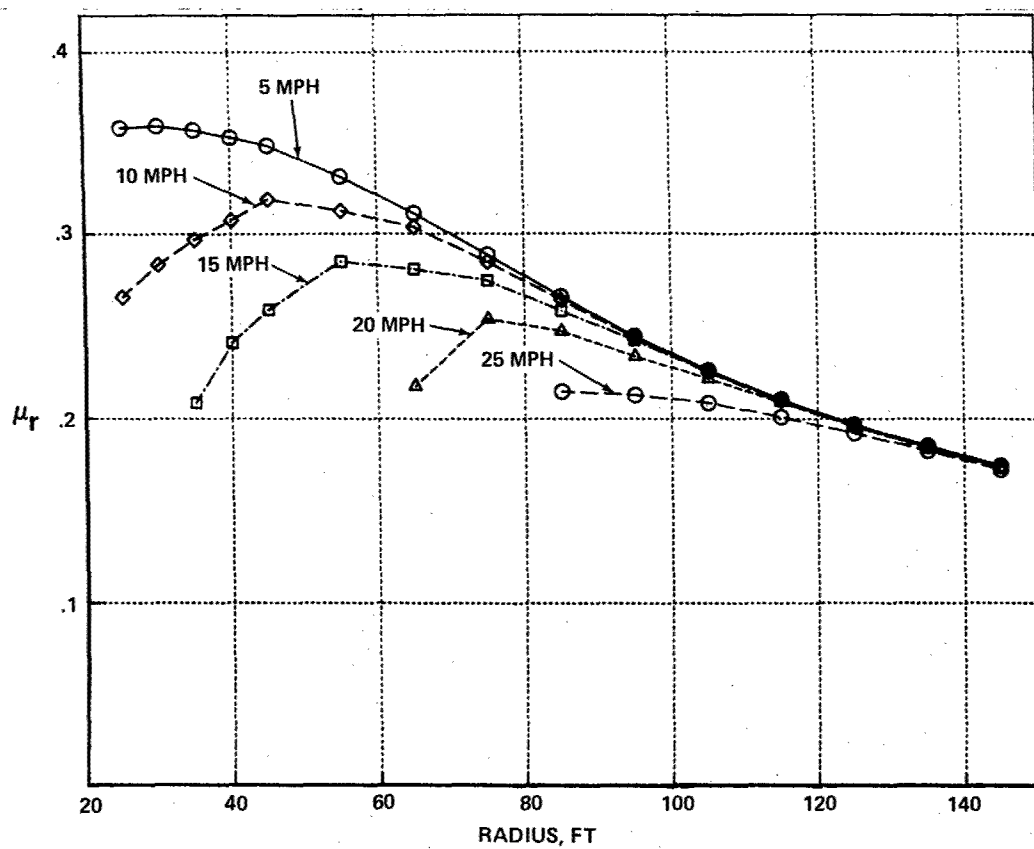
TABLE 3 - SELECTED SOIL CONDITIONS

1	Cohesive soil	CI = 24	c = 280 lb/sq ft	$\phi = 6^\circ$
2	Cohesive soil	CI = 53	c = 610 lb/sq ft	$\phi = 13.25^\circ$
3	Cohesionless soil		c = .1 lb/sq ft	$\phi = 35^\circ$

Figure 12 shows turning resistance coefficients calculated for the M60 tank as a function of turning radius for various velocities and soil conditions 2 in Table 3. Note that the turning resistance coefficient at various velocities approach the same envelope at some radius; this envelope represents the turning resistance at a low (hypothetically zero) speed. In the case shown in Fig. 12 the turning resistances at  $v = 5$  mph represent this envelope closely. The coefficient of turning resistance  $\mu_r$  decreases in various degrees at various speeds with the decrease of turning radius. Such a decrease indicates that less effort is needed to turn the vehicle at a higher speed than at a lower one. Although it would appear desirable to take advantage of this decrease and perform turning maneuvers at speeds where the resistance is reduced, the decrease of turning resistance is also indicative of the shear resistance of the soil at the track-soil interface being exceeded, a sign of incipient instability of steering.

If at a given radius and speed  $\mu_r$  is not indicated by its symbol in the figure, turning at that radius and speed is not possible because of skid out conditions.





0377-015W

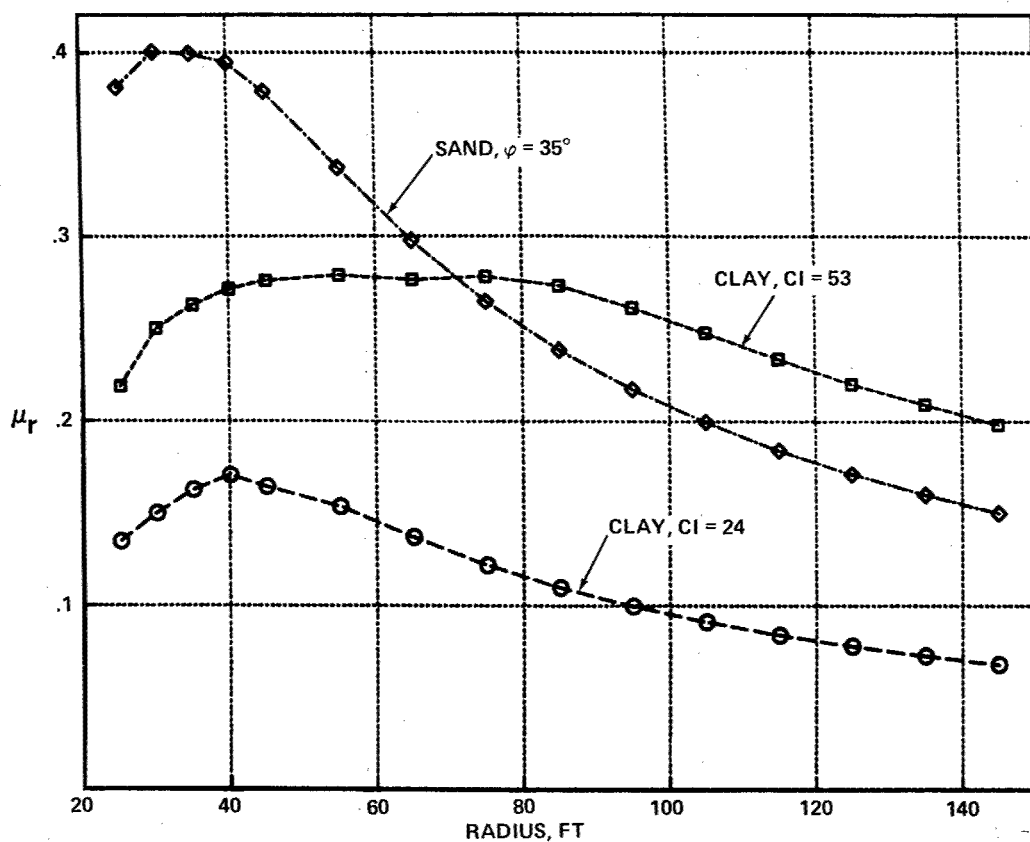
Fig. 12 Coefficient of Turning Resistance for M60 Tank at Various Speeds in Soil Condition 2

Figure 13 shows the variation of the coefficients of resistances of turning at 10 mph with the three selected soil conditions shown in Table 3, calculated for the M113 personnel carrier.

Note that in cohesive soil  $\mu_r$  increases with the strength of soil, since a stronger soil develops greater resistance to lateral movement than a weaker one. This is, of course contrary to what one would expect on the basis of common notions on motion resistance that decreases with soil strength. In turning, the advantage of greater soil strength manifests itself in the higher speed that can be achieved, provided that the vehicle is capable of developing the power required for turning. Attention is called to the very high coefficients of turning resistance calculated for sand. In general, cohesionless sands, prevalent in the Middle East, are more critical for turning, than cohesive (clay) soils.

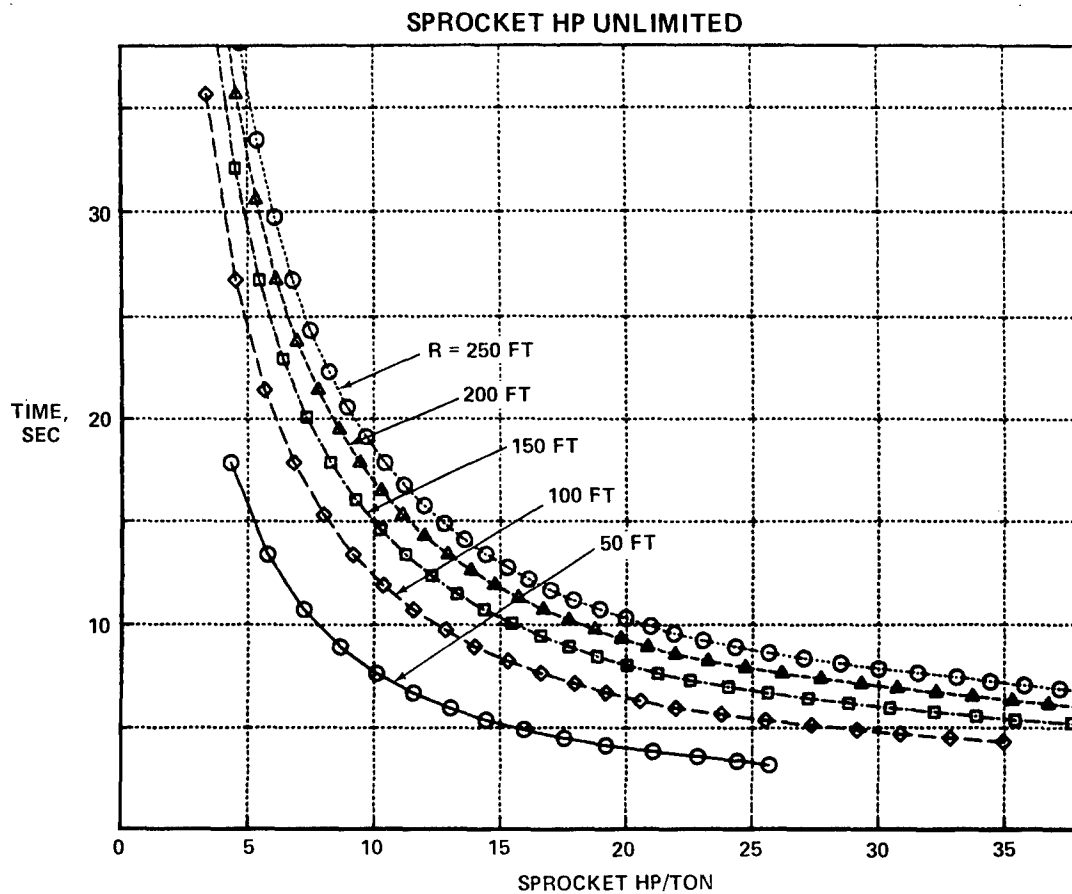
Another problem of interest is the relation between the time required for a vehicle to make a 90° turn and the sprocket horsepower required to make the turn. Figure 14 shows the results of such an analysis for the XM1 tank and soil conditions 2. The computations refer to steady state turns at various radii. The computed sprocket horsepower/ton values in the figure refer to sprocket horsepower values required to make the 90° turn irrespectively whether the power train in the vehicle is capable of providing that horsepower.

It has been noted in various field tests that the turning performance of tracked vehicles is noticeably different in a left turn from that in a right turn. One of the many sources of this different behavior is that the location of roadwheels on the left side is slightly offset from that on the right side. Since roadwheel distances from the cg are entered separately for the left and right side in the model, it is possible to analyze the effect of an offset on the turning performance. Figure 15 shows the results of such an analysis for the XM1 vehicle for soil conditions 2. The computed points almost coincide, indicating that the effect of the offset in roadwheel locations on turning performance is minimal.



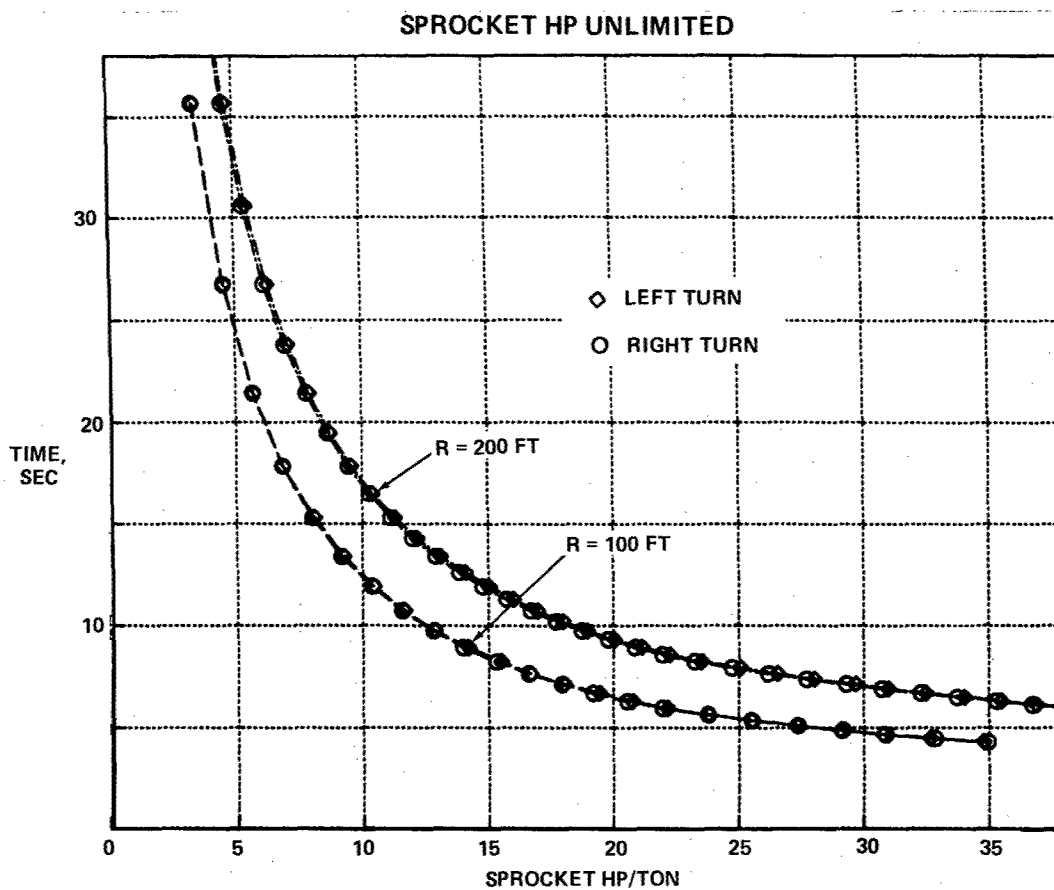
0377-016W

Fig. 13 Variation of Coefficient of Turning Resistance with Soil Conditions for M113 Vehicle at 10 mph



0377-017W

**Fig. 14 Time Required by the XM1 Tank to Make 90° Turns at Various Radii in Soil Condition 2**



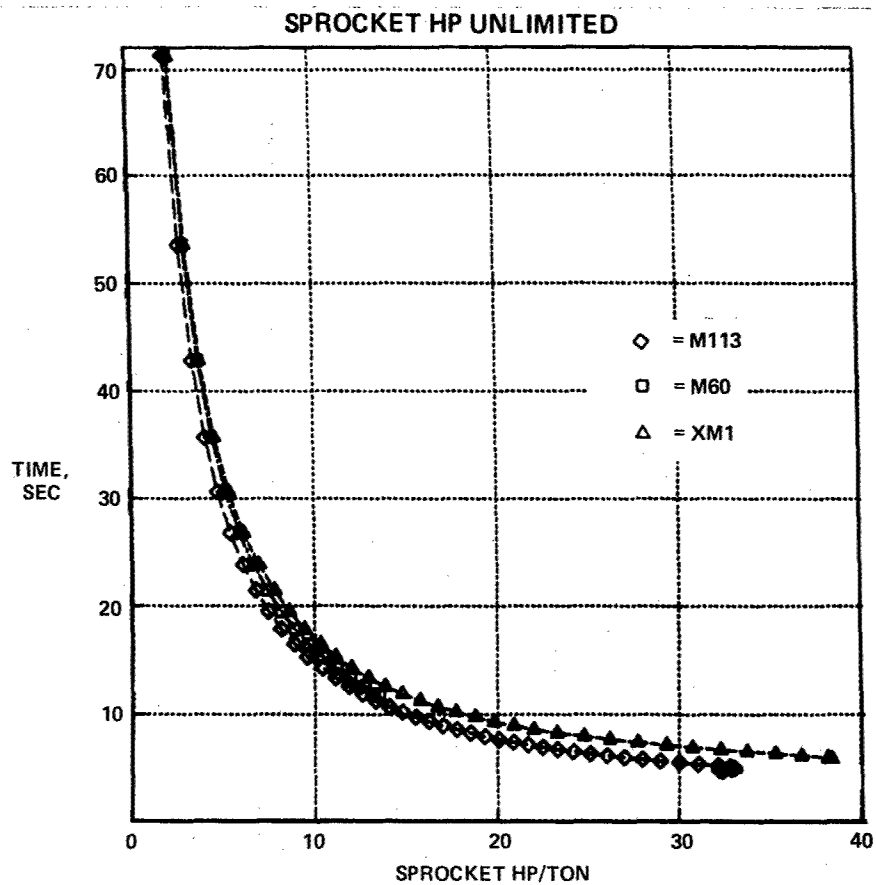
0377-018W

**Fig. 15 Time Required by XM1 Tank to Make 90° Left & Right Turns in Soil Condition 2**

Figure 16 shows a comparison of the time required to make a  $90^\circ$ ,  $R = 200$  ft turn by various vehicles. When plotted against sprocket horsepower/ton the computed time is comparable and not much different for the various vehicles. However, it should be emphasized that Fig. 16 shows only those differences in vehicle performance that are related to the interaction between the vehicle and soil. The sprocket horsepower/ton values refer to required values; power train and transmission models (not available at this time) would be needed to compare the expected actual performances of these vehicles. Internal resistance coefficients, that have a significant effect on horsepower requirements, have been assumed (in the absence of data) the same for all vehicles. Attention should be called, however, to the last point (going toward higher values of sprocket HP/ton) of the curves shown in the figure. The last point is controlled by vehicle-soil interaction; it indicates the shortest time the vehicle can make the  $90^\circ$  turn irrespectively of the available sprocket horsepower. It should be noted that the abscissas of the last point differ considerably for the various vehicles.

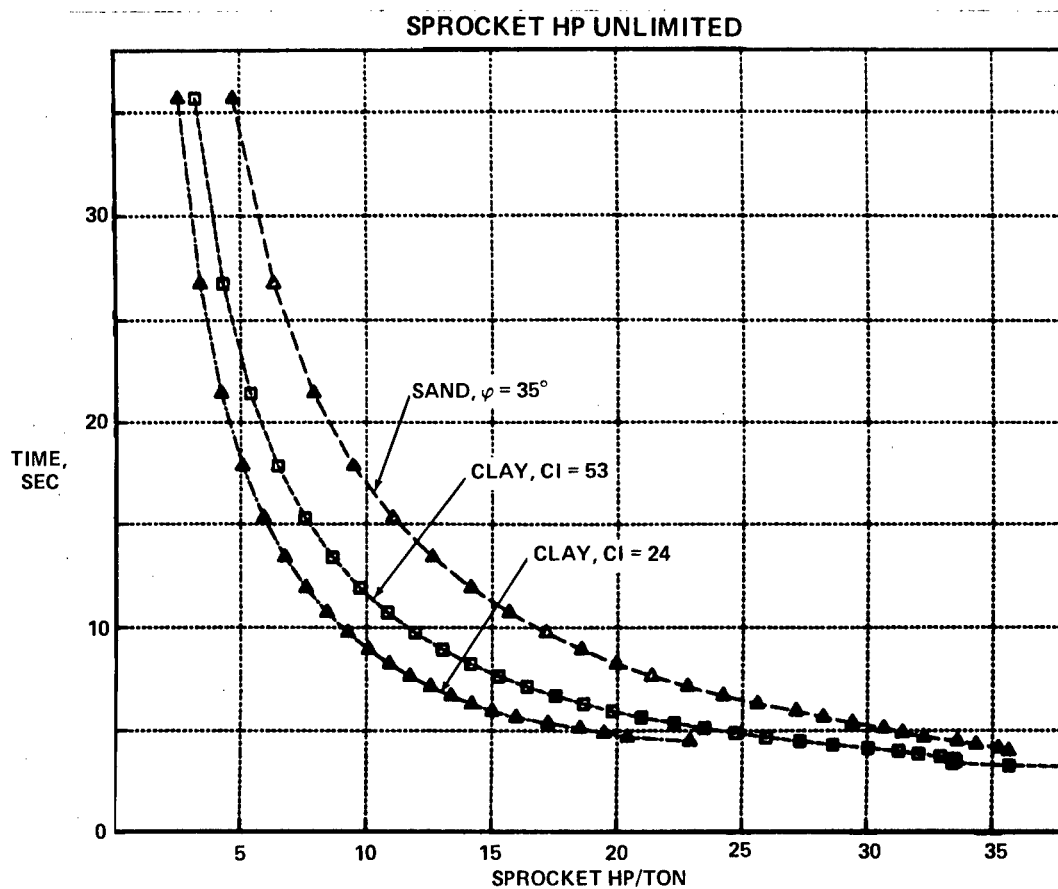
Figure 17 shows the time required by the M113 vehicle to make a  $90^\circ$ , 100 ft radius turn in various soils. It is seen that it is more difficult to negotiate such a turn in sand than in cohesive soils, a finding that has been confirmed by the results of numerous other analyses not presented here.

The model is also suitable for the determination of the maximum speed that vehicles can attain in steady state turns at various radii. This maximum speed may be controlled by either the soil conditions or the power requirements, therefore, a power train and transmission model is essential for the analysis of the maximum speed that vehicles can develop at various radii. Since at this time models of power transfer by the steering mechanism are not available, a simplified hyperbolic tractive force-speed relationship coupled with the Merritt powerloss formula applicable to the controlled differential steering of the M113 was used to estimate the sprocket horsepower available in turns at various speeds. Figure 18 shows the maximum speed calculated to be attainable by the M113 "Hotrod" in cohesive soil ( $C1 = 24$ ) at various radii together with maximum speeds obtained in field tests. Circles indicate the



0377-019W

**Fig. 16 Time Required by Various Vehicles to Make 90°, R = 200 ft Turn in Soil Condition 2**



0377-020W

**Fig. 17 Time Required by M113 Vehicle to Make 90° Turns in Various Soils**



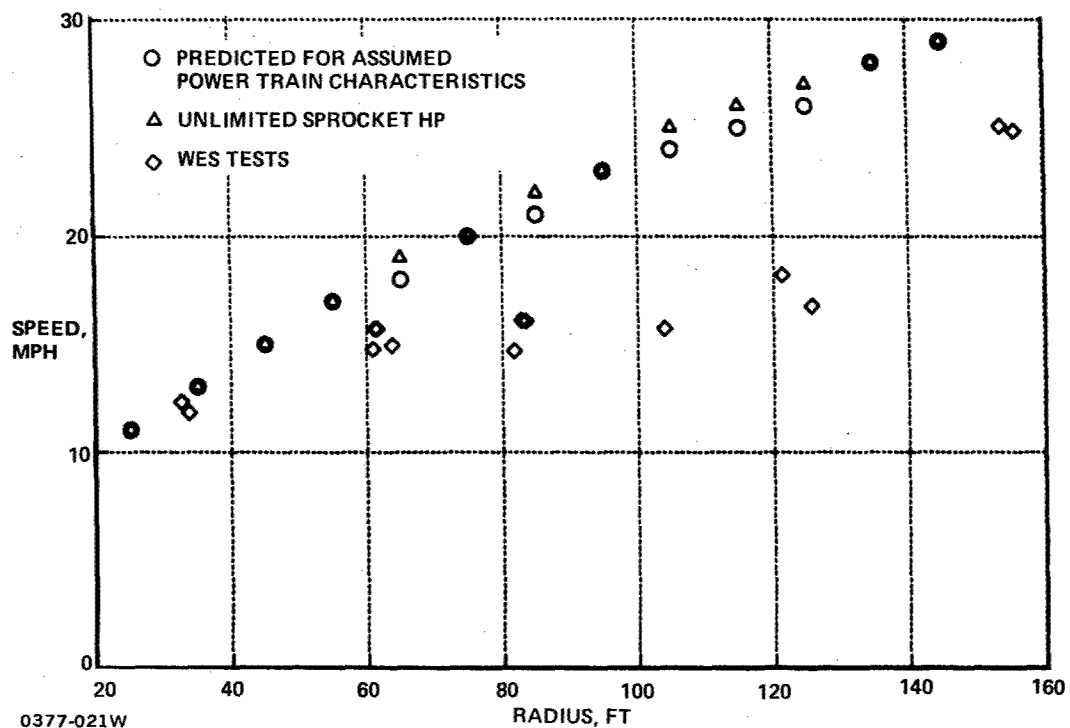


Fig. 18 Maximum Speed Attainable by "Hotrod" Version of M113 at Various Radii Under Soil Condition 2

maximum speed calculated with the simplified power train model, while triangles show the maximum speed on the condition that power is unlimited, i.e., the maximum speed that soil conditions allow. The discrepancy between calculated and observed speeds may very well be due to inaccuracies of the simplified power train model used.

Finally, the model is also suitable for the analysis of sinuous maneuvers, the path of which may be represented by the following equation

$$y = A \cos \left( \frac{\pi}{2} - 2\pi \frac{x}{L} \right) \quad (11)$$

where  $x$  = coordinate in the direction of travel

$y$  = offset

$A$  = amplitude

$L$  = length of a full cycle

The instantaneous radius of the sinuous path defined by Eq (10) is

$$R = \frac{[1 + A^2 \left(\frac{2\pi}{L}\right)^2 \sin^2 \left(\frac{\pi}{2} - 2\pi \frac{x}{L}\right)]^{3/2}}{-A \left(\frac{2\pi}{L}\right)^2 \cos \left(\frac{\pi}{2} - 2\pi \frac{x}{L}\right)} \quad (12)$$

It is assumed that the vehicle enters the path with some initial velocity then maintains that velocity as long as it is less than the maximum speed for steady state turn for the radius of curvature of the sinuous path. Then the vehicle travels at the maximum speed that soil conditions allow in steady state turn. These are shown in Fig. 19 for

$$L = 164 \text{ ft (50 m)}$$

$$A = 11.7 \text{ ft (3.57 m)}$$

$$V_e = 32 \text{ mph}$$

The maximum velocities shown in Fig. 19 refer to hypothetical steady state

UNLIMITED SPROCKET HP

ENTRY VELOCITY: 32 MPH

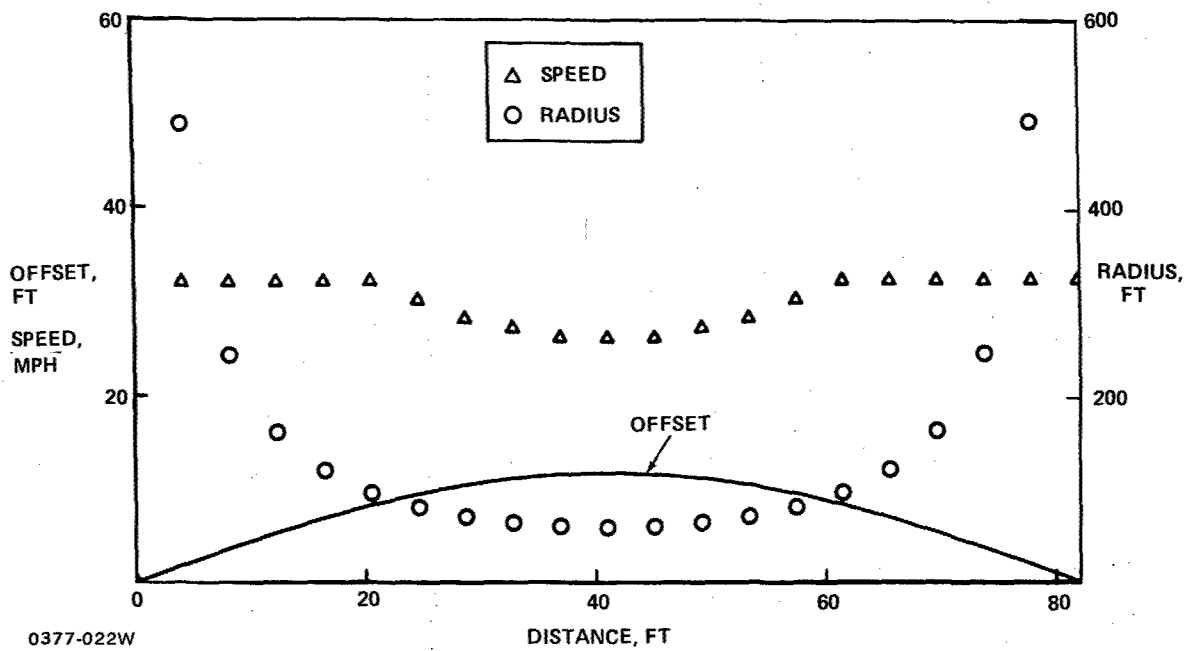
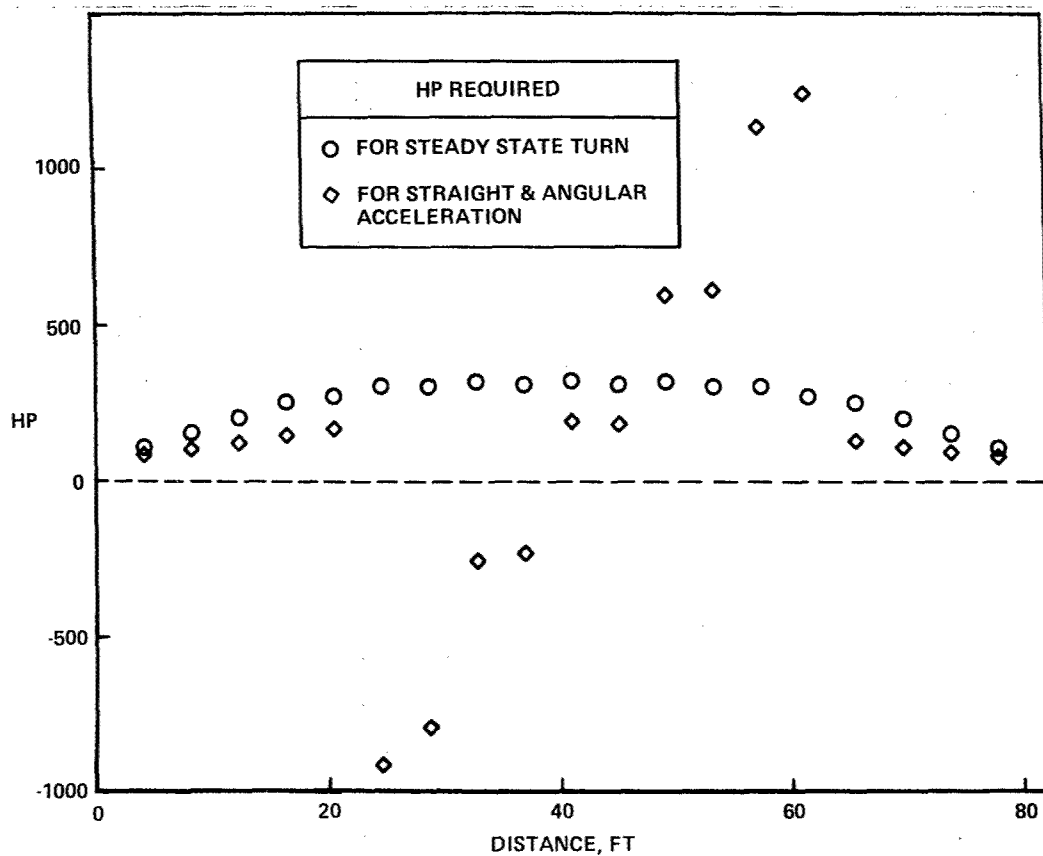


Fig. 19 Maximum Speed Along a Sinuous Path, Controlled by Steady State Turning About Instantaneous Radius of Curvature

turns at the instantaneous radius of curvature shown in the figure. These velocities, as well as the instantaneous radii change along the sinuous path involving not only deceleration and acceleration tangent to the path but also angular deceleration and acceleration about the yaw axis. The inertia forces resulting from these decelerations and accelerations affect the interaction of vehicle and soil in many ways. The steady state turning model does not account for these effects. However, the magnitude of power requirements for acceleration and power generation by deceleration for the path and velocities given in Fig. 19 have been calculated and are shown in Fig. 20. It is obvious that the excess power generated by the necessary deceleration of the vehicle to the max. speed possible at the smallest radius of curvature cannot be consumed even if both the outer and inner track were braked. The power required to accelerate the vehicle to regain the entry velocity at the end of the sine segment is an order of magnitude higher than that available in the M113. It is recommended that the present steady state turning model be further developed so as to incorporate simulation of transient interactions due to inertia forces.



0377-023W

**Fig. 20 Sprocket Horsepower Requirements for Sinuous Maneuver Shown in Fig. 19**

## 7 - CONCLUSIONS AND RECOMMENDATIONS

An analytical model for the simulation of the steady state turning of tracked vehicles in soft soil has been developed. The model is suitable for the determination of the following characteristics of turning performance as the function of soil conditions, turning radius and speed:

- o Coefficient of turning resistance
- o Time required to make 90° turns
- o Maximum speed at constant radius
- o Maximum speed along a sinuous path

These performance characteristics are essential for the evaluation of the agility of various vehicles and the power requirements associated with turning maneuvers. However, for more realistic simulation of non-steady evasive maneuvers it is recommended that the steady state model be further developed to allow for transient interactions due to inertia forces.

The analyses of turning performance conclusively indicate that cohesionless sand imposes the most severe conditions for turning. Field turning tests performed for the evaluation of the turning performance of tracked vehicles have been performed so far in cohesive clay soils only. Since in the strategically most important area of the Middle East sandy soils are prevalent, it is strongly recommended that field turning tests in sandy soils be performed. In view of the many variables that affect the turning performance it is also recommended that the analytical model be used in the development of the testing program for the purpose of establishing those testing conditions that are expected to yield the most information at the least cost. One of the objectives of the testing program would be the validation of the analytical model that would obviate further expensive field testing.

Internal track resistances contribute to the power requirements in turning significantly. Field measurements of motion resistance do not differentiate between internal and external resistances, therefore,

information on the magnitude of internal track resistances is scanty. It is recommended that field tests with instrumented track links be conducted that would allow the calculation of external resistances from the shear stresses acting on the track links.

## 8 - REFERENCES

1. Karafiath, L.L., "Track-Soil Interaction Model for the Determination of Maximum Soil Thrust," TARADCOM R & D Laboratory Technical Report No. 12380, July 1978.



DISTRIBUTION LIST  
(As of 1 January 1980)

Please notify USATARADCOM, DRDTA-ZSA, Warren, Michigan 48090, of corrections and/or changes in address.

Commander (25)  
US Army Tank Automotive  
Research and Development  
Command  
Warren, MI 48090

Superintendent (02)  
US Military Academy  
West Point, NY 10996

Attn: Dept of Engineering  
Course Director for  
Automotive Engineering

Commander (01)  
US Army Logistic Center  
Ft. Lee, VA 23801

Attn: ATCL-CC  
Mr. J. McClure

US Army Research Office (02)  
P.O. Box 12211  
Research Triangle Park, NC  
27709

Attn: Dr. Frederick W.  
Schmiedeshoff

Hq, DA (01)  
Washington, D.C. 20310

Attn: DAMA-ARZ-D  
Dr. Herschner

Hq, DA (01)  
Office of Dep Chief of Staff  
for Rsch, Dev & Acquisition  
Washington, D.C. 20310

Attn: DAMA-REZ-E  
Dr. Charles Church

Director (01)  
Defense Advanced Research  
Projects Agency  
1400 Wilson Boulevard  
Arlington, VA 22209

Commander (01)  
US Army Combined Arms Combat  
Developments Activity  
Ft. Leavenworth, KA 66027

Attn: ATCA-CCC-S

Commander (01)  
US Army Mobility Equipment  
Research and Development  
Command  
Ft. Belvoir, VA 22060

Attn: DRDME-RT

Commander (01)  
US Army Concept Analysis Agency  
Long Range Studies  
8120 Woodmont Avenue  
Bethesda, MD 20014

Dept of the Army (01)  
Office Chief of Engineers  
Chief, Military Program Team  
Research & Development Office  
Washington, D.C. 20314

Attn: DAEM-RDM

Director (02)  
US Army Corps of Engineers  
Waterways Experiment Station  
P.O. Box 631  
Vicksburg, MS 39180

Director (03)  
US Army Corps of Engineers  
Waterways Experiment Station  
P.O. Box 631  
Vicksburg, MS 39180

Attn: Mr. Nuttall

Director (04)  
US Army Cold Regions Research  
& Engineering Lab  
P.O. Box 282  
Hanover, NH 03755

Attn: Dr. Freitag,  
Dr. W. Harrison  
Dr. Liston  
Library

President (02)  
Army Armor and Engineer Board  
Ft. Knox, KY 40121

Commander (01)  
US Army Arctic Test Center  
APO 409  
Seattle, Washington 98733

Commander (02)  
US Army Test & Evaluation  
Command  
Aberdeen Proving Ground,  
Maryland 21005

Attn: AMSTE-BB and AMSTE-TA

Commander (02)  
Rock Island Arsenal  
Rock Island, IL 61201

Attn: SARRI-LR

Commander (02)  
US Army Yuma Proving Ground  
Yuma, Arizona 85364

Attn: STEYP-RPT, STEYP-TE

Mr. Frank S. Mendez, P.E. (01)  
Technical Director  
US Army Tropic Test Center  
Box 942  
Fort Clayton, Canal Zone 09872

Attn: STETC-TA

Commander (01)  
US Army Natick Laboratories  
Natick, Massachusetts 01760

Attn: Technical Library

Director (01)  
US Army Human Engineering Lab  
Aberdeen Proving Ground,  
Maryland 21005

Attn: Mr. Eckels

Director (02)  
US Army Ballistic Research Lab  
Aberdeen Proving Ground,  
Maryland 21005

Director (02)  
US Army Material Systems  
Analysis Agency  
Aberdeen Proving Ground,  
Maryland 21005

Attn: AMXSU-CM,  
Messrs. D. Woomert  
W. Niemeyer

Director (12)  
Defense Documentation Center  
Cameron Station  
Alexandria, Virginia 22314

US Marine Corps (01)  
Mobility & Logistics Division  
Development and Ed Command  
Quantico, VA 22134

Attn: Mr. Hickson

Naval Ship Research & Dev  
Center (01)  
Aviation & Surface Effects Dept  
Code 161  
Washington, D.C. 20034

Attn: E. O'Neal  
W. Zeitfuss

Director (01)  
National Tillage Machinery Lab  
Box 792  
Auburn, Alabama 36830

Director (01)  
USDA Forest Service Equipment  
Development Center  
444 East Bonita Avenue  
San Dimes, CA 91773

Director (01)  
Keweenaw Research Center  
Michigan Technological Univ  
Houghton, MI 49931

Engineering Societies (01)  
Library  
345 East 47th Street  
New York, New York 10017

Dr. M.C. Bekker (1)  
224 East Islav Drive  
Santa Barbara, CA 93101

Dr. I.R. Erlich (1)  
Dean for Research  
Stevens Institute of Tech  
Castle Point Station  
Hoboken, NJ 07030

Grumman Aerospace Corp (02)  
South Oyster Bay Road  
Bethpage, New York 11714

Attn: Dr. L. Karafiath  
Mr. F. Markow  
M/S A08/35

Dr. Bruce Liljedahl (01)  
Agricultural Engineering Dept  
Purdue University  
Lafayette, IN 46207

Dr. W.G. Baker (01)  
Dean, College of Engineering  
University of Detroit  
4001 W. McNichols  
Detroit, MI 48221

Mr. H.C. Hodges (01)  
Nevada Automtotive Test Center  
Box 234  
Carson City, NV 89701

Mr. R.S. Wismer (01)  
Deere & Company  
Engineering Research  
3300 River Drive  
Moline, IL 61265

Oregon State University (01)  
Library  
Corvallis, Oregon 97331

Southwest Research Inst (01)  
8500 Culebra Road  
San Antonio, TX 78228

Attn: Mr. R.C. Hemion

FMC Corporation (01)  
Technical Library  
P.O. Box 1201  
San Jose, CA 95108

Mr. J. Appelblatt (01)  
Director of Engineering  
Cadillac Gauge Company  
P.O. Box 1027  
Warren, MI 48090

Crysler Corporation (02)  
Mobility Research Laboratory,  
Defense Engineering  
Department 6100  
P.O. Box 751  
Detroit, MI 48231

Attn: Dr. B. VanDuesen  
Mr. J. Cohron

Library (01)  
CALSPAN Corporation  
Box 235  
4455 Benesse Street  
Buffalo, NY 14221

SEM, (01)  
Forsvarets forskningsanstalt  
Avd 2  
Stockholm 80, Sweden

Mr. Hedwig (02)  
RU III/6  
Ministry of Defense  
5300 Bonn, Germany

Foreign Science & Tech Ctr(01)  
220 7th Street North East  
Charlottesville, VA 22901

Attn: AMXST-GEI  
Mr. Tim Nix

General Research Corp (01)  
7655 Old Springhouse Road  
Westgate Research Park  
McLean, VA 22101

Attn: Mr. A. Viilu

Commander (01)  
US Army Development and  
Readiness Command  
5001 Eisenhower Avenue  
Alexandria, VA 22333

Attn: Dr. R..S. Wiseman

UNCLASSIFIED

SECURITY CLASSIFICATION OF THIS PAGE (When Data Entered)

REPORT DOCUMENTATION PAGE		READ INSTRUCTIONS BEFORE COMPLETING FORM	
1. REPORT NUMBER 12522	2. GOVT ACCESSION NO.	3. RECIPIENT'S CATALOG NUMBER	
4. TITLE (and Subtitle) Analytical Model for the Turning of Tracked Vehicles in Soft Soils		5. TYPE OF REPORT & PERIOD COVERED	
		6. PERFORMING ORG. REPORT NUMBER RE-	
7. AUTHOR(s) Leslie L. Karafiath		8. CONTRACT OR GRANT NUMBER(s) DAAK30-78-C-0080	
9. PERFORMING ORGANIZATION NAME AND ADDRESS Grumman Aerospace Corporation Research Department South Oyster Bay Road Bethpage, New York 11714		10. PROGRAM ELEMENT, PROJECT, TASK AREA & WORK UNIT NUMBERS	
11. CONTROLLING OFFICE NAME AND ADDRESS U.S. Army Tank Automotive Research and Development Command, Tank Automotive Concept Laboratory, DRDTA-ZSA, Warren, MI 48090		12. REPORT DATE October 1980	
		13. NUMBER OF PAGES 60	
14. MONITORING AGENCY NAME & ADDRESS (if different from Controlling Office)		15. SECURITY CLASS. (of this report)  UNCLASSIFIED	
		15a. DECLASSIFICATION/DOWNGRADING SCHEDULE	
16. DISTRIBUTION STATEMENT (of this Report)  Approved for public release; distribution unlimited			
17. DISTRIBUTION STATEMENT (of the abstract entered in Block 20, if different from Report)			
18. SUPPLEMENTARY NOTES			
19. KEY WORDS (Continue on reverse side if necessary and identify by block number) Inner track, interface friction angle, outer track, plasticity theory, slewing force, slip, speed, track force, turning, yaw center offset			
20. ABSTRACT (Continue on reverse side if necessary and identify by block number) An analytical model has been developed for the steady state turning of tracked vehicles in soft soils. The tracks of the vehicle are modeled by a series of rigid plates, each representing track links directly loaded by the roadwheels. The action of the track links in between the directly loaded ones is represented by a surcharge pressure. The soil is modeled by its Coulomb strength parameters; the interface between soil and track is characterized by the interface friction angle and slip. Track-soil interaction models have been developed separately for the outer track (driving mode) and inner track (braking			

mode), using plasticity theory for the determination of soil reactions. The slewing forces needed to overcome the turning resistances are determined iteratively. The yaw center offset is determined on the principle that it minimizes the turning resistance. Examples show the applications of the model for the determination of turning resistance, maximum speed of steady state turning and horsepower requirement for various military vehicles and soil conditions.